

## **AuPS/ASB Meeting - Newcastle 2007**

### **Free communications: Biophysics & spectroscopy**

Wednesday 5 December 2007 – Mulubinba Room

Chair: Brett Hambly

## **‘remedi’: Meeting the measurement needs of regenerative medicine**

*M.L. Mather, J.A. Crowe and S.P. Morgan, Applied Optics Group, School of Electrical & Electronic Engineering, University of Nottingham, Nottingham, NG7 2RD, UK. (Introduced by A. Collings)*

The next health care revolution will apply regenerative medicines using human cells and tissues (Langer *et al.*, 1999). Significant progress has been made towards the realisation of this, in particular, through the development of regenerative therapies for the treatment of diabetes, cartilage defects, wounds and bone defects (Griffith *et al.*, 2002). Whilst from a biological point of view, the therapeutic strategies of regenerative medicines are well defined there is a lack of commercial success (Mason, 2007; Lysaght *et al.* 2001). In addition to biological considerations, the production of regenerative therapies also requires consistent manufacturing and appropriate business and cost structures (Archer *et al.*, 2005). Remedi is a multidisciplinary consortium of UK-based universities and biotech companies which is addressing key challenges in regenerative medicine. These challenges are being met by combining the skills of a multidisciplinary team with the implementation of effective engineering strategies, both of which are integral to the establishment of regenerative medicine as a commercially viable, competitive industry.

The remedi consortium have expertise in: tissue engineering, economic modeling, policy and regulation relating to medical devices; machine platforms and sensor technology as well as production engineering that is necessary for the scale up of laboratory processes. Further, to ensure the commercial relevance of the program key inputs are received from industrial partners and a clinical advisory panel.

Central to the work of remedi is the application of effective engineering and manufacturing strategies for the scale up of regenerative medicines. This requires the economic production of functional therapies within a specification that satisfies both the regulator and clinical customer. In practice engineers and life scientists in the consortium are working together to analyse existing manufacturing systems utilising emerging measurement, sensing and control techniques to re-engineer and scale-up current laboratory bench-based processes. This requires each stage in the process to be sufficiently robust and reproducible. Further, each stage must be well characterised and its impact on the resulting product well understood.

This paper reports the role measurement and sensing systems are playing to expedite the scale-up of regenerative therapies. This work describes three case studies, tissue scaffold fabrication, cell culture and tissue engineering, in which greater process understanding can be obtained through the application of measurement and engineering principles. Specifically, time-lapsed imaging and acoustic impedance monitoring are applied to in-process monitoring of tissue scaffold fabrication. Scanning electron microscopy, micro x-ray computed tomography, magnetic resonance imaging and terahertz pulsed imaging are utilised to characterise scaffolds post-fabrication. An automated cell culture platform is used to facilitate identification of key environmental factors affecting cell culture. Further, the measurement challenges associated with non-destructive characterisation of engineered tissue are demonstrated through characterisation of a dermal skin substitute with optical spectroscopy.

This work concludes that there is a need for a greater emphasis on the engineering and manufacturing issues related to regenerative therapies if commercial viability is to be realised. In particular, attention needs to be paid to: improving process and system design in tissue production; implementing process monitoring in all stages of the therapy production; and improving strategies for preservation of final products and product release. This work demonstrates that the principles of design, measurement and process monitoring from the physical sciences will be integral to the translation of regenerative therapies into the clinic and that much of the technology needed to realise this is already available.

Archer R & Williams DJ (2005) *Nature Biotechnology*, **23**: 1353-5.

Griffith LG & Naughton G. (2002) *Science*, **8**: 1009-14.

Langer RS & Vacanti JP. *Scientific American*, **280**: 86.

Lysaght MJ & Hazlehurst AL. (2001) *Tissue Engineering*, **10**: 309-20.

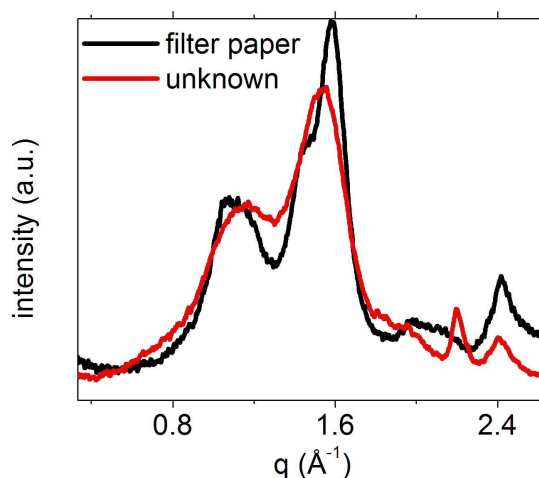
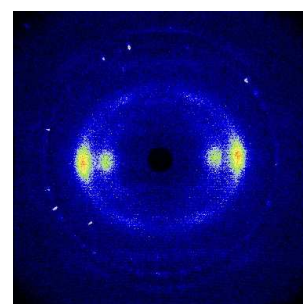
Mason C. (2007) *Medical Device Technology*, **March/April**: 25-28.

## X-ray diffraction as a tool to study the arrangement of cellulose molecules in plant cell walls

C.J. Garvey,<sup>1</sup> O. Paris<sup>2</sup> and R. Gillespie,<sup>3</sup> <sup>1</sup>ANSTO, PMB 1, Menai, NSW 2234, Australia, <sup>2</sup>Max Planck Institute of Colloids and Interfaces, Department of Biomaterials, 14424 Potsdam, Germany and <sup>3</sup>Department of Archaeology and Natural History, Australian National University, ACT 0200, Australia.

Cellulose, the primary structural polymer in plant cell walls, is unique among polymers utilised by man in its simultaneous synthesis of the polymer and primary unit of nanoscale arrangement, the microfibril. In contrast with the technological world, the plant kingdom achieves diverse mechanical functionality simply by modulating the nanoscale arrangement of cell wall polymers, by the arrangement of cellulose microfibrils. Because of its suitability for spatially localised *in situ* measurements, we have used wide angle x-ray diffraction (WAXD) patterns to investigate the nanoscale arrange of cellulose in microfibrils (Garvey *et al.*, 2005; Garvey *et al.*, 2006) and in oriented samples with respect to applied forces (Martinschitz *et al.*, 2006). Microfibrils are composed of an integral number of cellulose chains, and the number and thus the size of the microfibril are characteristic of the botanical origin of the cellulose. These studies apply a pure size broadening approach to the interpretation of cellulose X-ray diffraction peaks (Garvey *et al.*, 2005). Here we report WAXD area detector data, shown in the image, from plant material presumed to be the gut contents of an extinct giant marsupial, *Diprotodon opatum*, excavated from Lake Callabonna, South Australia (Stirling, 1894).

The two-dimensional anisotropic WAXD data has been radially averaged around the x-ray, centre of the image, to produce a one-dimensional representation, shown in the graph. Using a Voigt function to approximate size broadening of cellulose diffraction peaks we speculate on the putative diet of this animal, based on comparison with size broadening of diffractions peaks of material from modern plants (from the same region), and other sources of cellulose. While these observations give clues to the diet of this giant extinct marsupial, they also give interesting insights into the interpretation of WAXD from cellulose, and ultimately will help us exploit this renewable and versatile material, cellulose.



Garvey CJ, Keckes J, Lee G, Parker IH & Beilby M. (2006) *Cryptogamie Algologie*, **27**: 391-401.

Garvey CJ, Simon GP, & Parker IH (2005) *Macromolecular Chemistry and Physics*, **206**: 1568-1575.

Martinschitz KJ, Boesecke P, Garvey CJ, Gindl W & Keckes J. (2006) *Journal of Material Science*, DOI: 10.1007/s10853-006-1237-7.

Stirling EC. (1894) *Nature*, **50**: 184-188.

## **Novel signalling in mouse embryonic stem cells alters the pluripotent state**

A.C. Lonic,<sup>1</sup> F. Felquer,<sup>2</sup> N. Hamra<sup>2</sup> and M.B. Morris,<sup>3</sup> <sup>1</sup>*Institute of Medical and Veterinary Science, Adelaide, SA 5000, Australia, <sup>2</sup>School of Biomedical Science, University of Adelaide, Adelaide, SA 5000, Australia and <sup>3</sup>Human Reproduction Unit, School of Medical Sciences, University of Sydney, NSW 2006, Australia.*  
(Introduced by Derek Laver)

The phenotypic status of embryonic stem (ES) cells is controlled in part by signalling pathways which translate inputs by extracellular molecules. An important extracellular protagonist in mouse ES cells is LIF (leukaemia inhibitory factor) which interacts with the gp130/LIFR membrane-receptor complex to activate a number of downstream signalling arms, including the STAT3, MEK/ERK and PI3K/Akt pathways. These pathways, together with others, interact in complex and sometimes competing ways to generate the well-known phenotypic characteristics of mouse ES cells of self-renewal, high rates of proliferation, and pluripotency.

The addition of a second molecule, L-proline, to the extracellular environment alters the pluripotent status of mouse ES cells, converting them to a second pluripotent cell population equivalent to the primitive ectoderm of the pre-gastrulating embryo. This conversion, from ES cells to primitive ectoderm-like cells, primes the latter for directed differentiation to specific cell types (Bettess *et al.*, 2003). Here we show, using inhibitor studies and kinome array analysis, that this small molecule appears to work by i) changing the balance in activity of signalling pathways already stimulated by LIF, and ii) activating additional signalling pathways. Specifically, L-proline rapidly further activates the LIF-stimulated MEK/ERK pathway, tipping the balance in favour of differentiation and away from ES-cell self-renewal sustained by LIF-mediated activation of the STAT3 pathway. In addition, L-proline rapidly stimulates other pathways including p38, mTOR and PI3K/Akt each of which contributes, to a greater or lesser extent, to the conversion to primitive ectoderm-like cells.

These results indicate that through the addition of small, nontoxic activators and inhibitors of signalling pathways, the differentiation of pluripotent ES cells might be controlled sufficiently well for the homogeneous production of specific cell types suitable for use in animal models of human disease.

Bettess MD, Lonic A, Washington JM, Lake JA, Morris MB, Rathjen J & Rathjen PD. (2003) *Proceedings of the 1<sup>st</sup> Australian National Stem Cell Conference*, p229.

## Does *N*-acetylcysteine act as an intracellular cysteine precursor in human erythrocytes?

J.E. Raftos,<sup>1</sup> S. Whillier<sup>1</sup> and P.W. Kuchel,<sup>2</sup> <sup>1</sup>Department of Biological Sciences, Macquarie University, NSW 2109, Australia and <sup>2</sup>School of Molecular and Microbial Biosciences, University of Sydney, NSW 2006, Australia.

In sickle cell disease haemoglobin S oxidises at a rate of 6% per day releasing reactive oxygen species that reduce the concentration of the important antioxidant glutathione (GSH). Oral administration of *N*-acetylcysteine (NAC) has been shown to increase the GSH concentrations in sickle red blood cells (RBCs). RBCs with higher GSH concentrations are less likely to become irreversibly sickled and patients with low populations of irreversibly sickled RBCs have fewer vaso-occlusive episodes (Pace *et al.*, 2003). GSH is synthesized from glutamate, cysteine and glycine and in RBCs the rate of synthesis is controlled by feedback inhibition of GSH. When RBCs are depleted of GSH, the supply of cysteine from the plasma becomes rate limiting. It has been assumed that on oral administration NAC enters the RBCs where it is deacetylated to release the cysteine required for GSH production. The aim of this study was to determine whether this was in fact the mode of action of NAC.

*In vitro*, both extracellular cysteine and NAC can provide a source of cysteine for GSH production in RBCs that have been depleted of 80% of their initial GSH concentration by incubation with 1-chloro-2,4-dinitrobenzene. However, while 1.0 mM NAC was required for the maximum rate of GSH synthesis cysteine at only 60  $\mu$ M supported synthesis at the same rate (Raftos *et al.*, 2007). To determine why NAC was a relatively inefficient cellular cysteine precursor, we measured the kinetics of the uptake and deacetylation of NAC.

GSH depleted RBCs were incubated in a range of extracellular NAC concentrations up to 10 mM and NAC uptake was measured as the initial rate of increase in total RBC thiols. Uptake did not approach saturation at 10 mM extracellular NAC and the first order rate constant was  $2.04 \pm 0.07 \text{ min}^{-1}$ . When the experiment was repeated with 50  $\mu$ M DNDS or 5  $\mu$ M DIDS, NAC uptake was inhibited by 58% indicating that the majority of the NAC enters by low affinity transport via the anion exchange protein. This is not surprising as NAC carries a negative charge at plasma pH. The  $K_m$  and  $V_{max}$  for deacetylation of NAC measured using <sup>1</sup>H NMR in concentrated RBC haemolysates were  $1.49 \pm 0.16 \text{ mM}$  and  $1.61 \pm 0.018 \mu\text{mol L}^{-1} \text{ min}^{-1}$ , respectively (Raftos *et al.*, 2007). Oral NAC at the dosage sufficient to increase GSH concentration in the RBCs of sickle cell patients produces a plasma concentration of only 10  $\mu$ M while free cysteine increases by 50  $\mu$ M (Burgunder *et al.*, 1989). At this concentration the measured rates of uptake and deacetylation of NAC are too slow to supply intracellular cysteine rapidly enough to maintain GSH synthesis. We conclude that NAC acts in the plasma by breaking thiol bonds to replace bound cysteine. The freed plasma cysteine can then enter the RBCs to support GSH synthesis.

- Burgunder JM, Varriale A & Lauterburger BH. (1989) *European Journal of Clinical Pharmacology*, **36**: 127-31.  
Pace BS, Shartava A, Pack-Mabien A, Mulekur M, Ardia A & Goodman SR. (2003) *American Journal of Hematology*, **73** 26-32.  
Raftos JE, Whillier S, Chapman BE & Kuchel PW. (2007) *International Journal of Biochemistry and Cell Biology*, **39**: 1698-1706.

## Free energy simulations of potassium channels - KcsA, Shaker and HERG

*S. Kuyucak and T. Bastug, School of Physics A28, University of Sydney, NSW 2006, Australia.*

There are by now several potassium channel structures available both in the open and closed states. Using these structures in free energy molecular dynamics simulations, it is possible to study the structure-function relations in potassium channels in a rigorous fashion. Here we use free energy simulations in a comparative study of KcsA, Shaker and HERG potassium channels. Some of the issues to be considered are:

i) Role of the cmap terms in the CHARMM force field in stabilizing the structure of the selectivity filter: The cmap dihedral terms are relatively new addition to the CHARMM force field. We find that these terms play an essential role in keeping the C=O carbonyl dipoles in the selectivity filter directed towards the channel axis as observed in the crystal structures of potassium channels, and necessary for providing a complete hydration shell for the permeating K<sup>+</sup> ions.

ii) Comparison of the filter structures in KcsA, Shaker and HERG channels: KcsA is known to have a very stable filter structure, which leads to a large selectivity margin for permeation of K<sup>+</sup> vs Na<sup>+</sup> ions. Loss of the some of the H-bonds in other potassium channels results in a less selective channel, e.g., in HERG channel, K/Na selectivity is completely lost due to the flexibility of the S1 binding site. Nevertheless selectivity is retained in the other (S2-S4) binding sites.

iii) Energetics of ion permeation in KcsA and Shaker channels from potential of mean force (PMF) calculations: It is well established that 3 K<sup>+</sup> ions can occupy the S0, S2 and S4 sites in the KcsA channel.

Here we demonstrate that this is the only stable configuration for 3 K<sup>+</sup> ions in the filter by constructing PMF's of a K<sup>+</sup> ion while the filter is occupied by other 2 K<sup>+</sup> ions. A much higher PMF is found when the two K<sup>+</sup> ions are at the S1-S3 sites compared to that of S0-S2, which indicates that simultaneous occupation of the S1, S3, and S4 sites is not energetically feasible. Similar PMF results are obtained for the corresponding PMF calculations in the Shaker filter, reinforcing the homology of the filter structures among the potassium channels from the bacterial to the mammalian.

## **In vivo measurement of hepatic lipid composition by proton magnetic resonance spectroscopy**

N.A. Johnson,<sup>1</sup> D.W. Walton,<sup>2</sup> T. Sachinwalla,<sup>2</sup> C.H. Thompson,<sup>3</sup> K. Smith,<sup>1</sup> P. Ruell,<sup>1</sup> S.R. Stannard<sup>4</sup> and J. George,<sup>5</sup> <sup>1</sup>Discipline of Exercise and Sport Science, The University of Sydney, East Street, Lidcombe, NSW 2141, Australia, <sup>2</sup>Department of Magnetic Resonance, Rayscan Imaging, 41-43 Goulburn Street Liverpool, NSW 2170, Australia, <sup>3</sup>Department of Medicine, Flinders University, Bedford Park, SA 5042, Australia, <sup>4</sup>Institute of Food, Nutrition and Human Health, Massey University, Palmerston North Private Bag 11222, New Zealand and <sup>5</sup>Storr Liver Unit Westmead Millennium Institute, The University of Sydney, Westmead Hospital, Westmead, NSW 2145, Australia.

Non-alcoholic fatty liver is frequently observed in obese individuals, yet the factors which predict its development and progression to liver disease are poorly understood. It has been proposed that an increase in hepatic saturated fatty acids and/or a decrease in polyunsaturated fatty acids predisposes to hepatic triglyceride accumulation and inflammation.

We assessed the efficacy of using proton magnetic resonance spectroscopy (<sup>1</sup>H-MRS) to non-invasively measure hepatic lipid composition. Hepatic lipid unsaturation index (UI), a surrogate saturation index (SI) and polyunsaturation index (PUI) measured by <sup>1</sup>H-MRS were in agreement with those expected in oils of known composition. Hepatic triglyceride concentration (HTGC) and composition were then measured *in vivo* in healthy lean (LEAN) men ( $n = 10$ ), obese men with normal HTGC (OB) ( $n = 8$ ) and obese men with hepatic steatosis (OB+HS) ( $n = 9$ ).

HTGC was significantly higher in OB+HS ( $14.9 \pm 3.2$  %) versus OB ( $2.4 \pm 0.4$  %) and LEAN ( $0.4 \pm 0.1$  %) (Figure A;  $p < 0.01$  for both). SI was significantly higher in OB+HS ( $0.94 \pm 0.01$ ) and OB ( $0.91 \pm 0.01$ ) versus LEAN ( $0.80 \pm 0.02$ ) (Figure B;  $p < 0.01$  for both). PUI was significantly lower in OB+HS ( $0.003 \pm 0.001$ ) and OB ( $0.029 \pm 0.001$ ) versus LEAN ( $0.102 \pm 0.013$ ) ( $p < 0.01$ ), and significantly lower in OB+HS versus OB (Figure C;  $p < 0.05$ ).

These findings demonstrate that hepatic lipid composition can be non-invasively measured by <sup>1</sup>H-MRS, and that obese men with and without hepatic steatosis exhibit a significant increase in SI and a decrease in PUI when compared with healthy lean men. Furthermore, obese men with hepatic steatosis showed specific depletion of polyunsaturated fatty acids (PUFAs) when compared with obese men with normal HTGC. These data are consistent with those derived by needle biopsy and histology by Araya *et al.* (2004). While a cause-effect relationship cannot be inferred from our cross-sectional research design, our finding is consistent with the postulation that dilution of hepatic lipid PUFAs promotes triglyceride accumulation by reducing triglyceride export and inhibiting lipid oxidation (Videla *et al.*, 2004). Further longitudinal research is required to confirm this hypothesis and the suggestion that this phenotype might further predispose to inflammation (Videla *et al.*, 2004).

Araya J, Rodrigo R, Videla LA, Thielemann L, Orellana M, Pettinelli P & Poniachik J. (2004) *Clinical Science*, **106**: 635-643.

Videla LA, Rodrigo R, Araya J & Poniachik J. (2004) *Free Radical Biology and Medicine*, **37**: 1499-1507.

